Wind and Structures, *Vol. 21, No. 1 (2015) 1-23*
DOI: http://dx.doi.org/10.12989/was.2015.21.1.001

Wind pressure characteristics of a low-rise building with various openings on a roof corner

Yunjie Wang[1] and Q.S. Li*[2]

[1]*College of Civil Engineering, Hunan University, Changsha 410082, P.R. China*
[2]*Department of Architecture and Civil Engineering, City University of Hong Kong, Kowloon, Hong Kong*

(Received September 27, 2014, Revised February 5, 2015, Accepted February 19, 2015)

Abstract. Wind tunnel testing of a low-rise building with openings (holes) of different sizes and shapes on a roof corner is conducted to measure the internal and external pressures from the building model. Detailed analysis of the testing data is carried out to investigate the characteristics of the internal and external pressures of the building with different openings' configurations. Superimposition of the internal and external pressures makes the emergence of positive net pressures on the roof. The internal pressures demonstrate an overall uniform distribution. The probability density function (PDF) of the internal pressures is close to the Gaussian distribution. Compared with the PDF of the external pressures, the non-Gaussian characteristics of the net pressures weakened. The internal pressures exhibit strong correlation in frequency domain. There appear two humps in the spectra of the internal pressures, which correspond to the Helmholtz frequency and vortex shedding frequency, respectively. But, the peak for the vortex shedding frequency is offset for the net pressures. Furthermore, the internal pressure characteristics indirectly reflect that the length of the front edge enhances the development of the conical vortices.The objective of this study aims to further understanding of the characteristics of internal, external and net pressures for low-rise buildings in an effort to reduce wind damages to residential buildings.

Keywords: low-rise building; wind tunnel testing; wind loading; internal pressure; external pressure; net pressure; separation bubble; conical vortex

1. Introduction

Low-rise building is one of the most ubiquitous architectural forms. Windstorm-induced disasters cause significant economic losses and heavy causalities throughout the world almost every year, most of which result from the collapse or damage of low-rise residential buildings. A number of post-disaster surveys (van de Lindt *et al*. 2007) showed that the wind-induced damages mainly occurred on low-rise buildings. Therefore, the effects of wind on low-rise buildings have received a great deal of attention in the past. Field measurements (Li *et al*. 2010, Kopp and Morrison 2012, Li *et al*. 2012, Tecle *et al*. 2013) and experimental model studies (Zhao 1997, Kawai 2002, Mahmood 2011) showed that low-rise buildings suffer extremely large suctions at the windward corners and leading edges on buildings' roofs. It has been recognized that much of the damage to low-rise buildings has been caused by such large suctions on buildings' roofs. The

*Corresponding author, Professor, E-mail: bcqsli@cityu.edu.hk

http://www.techno-press.org/?journal=was&subpage=8 ISSN: 1226-6116 (Print), 1598-6225 (Online)

primary damage patterns of low-rise buildings under windstorms include overturning of sheathings on roof corners, roof edges and ridges, as well as structural destroy of a whole roof. The previous researches partially revealed the mechanisms of the devastating effects and provided the basis for the wind-resistant design of low-rise buildings.

It has been noticed that the damage to a low-rise building is related to the internal pressure in the building with a dominant opening. Extensive research works on this topic have been conducted, which mainly considered a dominant opening on the windward wall of a house (Holmes 1979, Liu and Saathoff 1981, Stathopoulos and Luchian 1989, Vickery and Bloxham 1992, Ginger *et al*. 1997, Tecle *et al*. 2013, Sharma 2013). Through wind tunnel experiments of the TTU building model with a dominant hole on the windward wall, Sharma and Richards (2003) discussed the Helmholtz resonance phenomenon for incident wind flows from different wind directions and the application of the quasi-steady approach to the internal pressure. Recently, Pan *et al.* (2013) studied the wind-induced internal pressures when there were multiple openings on walls of a low-rise building. They recommended that the positions of the holes (openings) should be taken into account when predicting the potential wind-caused damages to low-rising buildings. By changing different combinations of wall openings and background leakages, Guha *et al.* (2011) investigated the internal pressure dynamics of a leaky building with a dominant opening.

A few previous studies considered the cases that there were central openings on roofs of low-rise buildings (Huang and Gu 2004, Blocken and Persoon 2009). However, literature survey revealed that an important case that there are openings located on a roof corner of a low-rise building has not been considered in the previous studies. In view of this, this paper investigates the characteristics of internal and external pressures for a low-rise building with openings on a roof corner through wind tunnel testing. By changing the sizes and shapes of the openings in the wind tunnel experiment, we aim to simulate different failure stages until the destroyed situation of the roof corner to study the associated internal, external and net pressures.

2. Wind tunnel testing

2.1 Experimental model

An experimental model with length scale ratio of 1:10 was made for the wind tunnel testing, corresponding to the prototype low-rise building with 6m length, 4m width and 4m height. This full-scale building with flat roof was an instrumental experimental building for monitoring the wind effects on it. The experimental building was built by Li *et al.* (2012) which provided the introduction on the experimental building and the associated full-scale measurements. Different cases of the openings on the model were considered in the wind tunnel testing. Case Ⅰ has a rectangular hole with sizes of 100 mm×100 mm on a roof corner. At each measuring point on the model, two pressure taps were mounted on the external surface and the internal side. In other words, at each measuring point, the external pressure and internal pressure were measured simultaneously in the wind tunnel testing. The distribution and number of pressure taps in conjunction with the definition of wind direction are shown in Fig. 1(a). There are six taps on the inside and outside walls perpendicular to 0° wind direction (Fig. 1(b)). Other cases, through changing the sizes and shapes of the openings by cover plates, are exhibited in Figs. 1(c)-1(f).

In order to satisfy the requirement that the ratio of internal fluctuating frequency to external fluctuating frequency should be similar for the wind tunnel testing and the prototype, the model

cavity volume and the prototype cavity volume should fulfill the following formula (Holmes *et al.* 2012)

$$\frac{V_m}{V_p} = \frac{\left(l_m / l_p\right)^3}{\left(U_m / U_p\right)^2} \tag{1}$$

where, V is the internal cavity volume, l is the geometric length, U is the mean wind speed, subscript m and p represent model and prototype, respectively. Hence, the volume of the model should be enlarged by the square of the speed ratio, on condition that the external geometrical shape of the building should not be changed, which can be realized by increasing the cavities at the bottom of the model.

2.2 Wind flow simulation

Wind tunnel experiment was conducted at the Key Laboratory of Building Safety and Energy Efficiency of the Ministry of Education of China in Hunan University. During the testing, wind speed was kept to be 10 m/s at the reference height (the roof height of the building model). The model was placed at the center of the turntable in the wind tunnel. Fig. 2 shows the building model in the wind tunnel. Wind direction varied from 0° to 90° with an interval of 5° in the wind tunnel testing. By arranging wedges and cubic rough elements in front of the model, wind flow field over the terrain of Category B (open terrain) specified in the Chinese load code (GB50009-2012) was simulated for the model testing. Without the model placed at the turntable, the simulated mean wind speed profile, turbulence intensity profile and spectrum in the longitudinal direction are demonstrated in Fig. 3, in which *Ur* represents the mean wind speed at the reference height, *U* is the mean wind speed at height *z*, *Sv* is the spectral amplitude of the longitudinal wind speed, *f* is the frequency, *H* is the reference height, and σ is the standard deviation of the longitudinal wind speed.

2.3 Data processing

In the experiment, the sampling frequency was 312.5Hz and the sampling time was 32 seconds. There were 10000 pressure data recorded from each pressure tap for an incident wind direction during the testing. The pressures were converted into non-dimensional pressure coefficients by the following equation.

$$Cp_i(t) = \frac{P_i(t) - P_\infty}{1/2\,\rho U_H^2} \tag{2}$$

where, $C_{pi}(t)$ refers to the time series of wind pressure coefficient at tap i, $P_i(t)$ is the time series of wind pressure at tap i, P_∞ is the reference static pressure, ρ is the air density and takes the value of 1.25 kg/m^3 according to the Chinese load code, U_H is the longitudinal mean wind speed at the reference height (the roof height). The net pressure coefficients at tap i, on the model are calculated by the following equation.

$$Cp_{ni}(t) = \frac{P_{ui}(t) - P_{di}(t)}{1/2\,\rho U_H^2} \tag{3}$$

where, $C_{pui}(t)$ is the time series of net pressure coefficient, $P_{ui}(t)$ and $P_{di}(t)$ are the time series of internal and external wind pressures at tap i, respectively. In addition, there was a convention in this paper that pressure along the outer surface normal vector was negative, or else, pressure was positive.

3. Analysis of testing data

3.1 Characteristics of wind pressure distributions on the roof

When the incident flow is perpendicular to the ridge of the building, there forms a separation bubble on the roof due to the flow separation and reattachment. As the incident wind attacks the building in an oblique direction, one or a pair of conical vortices comes into being because of flow separation along the windward edges of the roof (Wu 2000). Figs. 4 and 5 respectively display the distributions of the mean pressure coefficients and root-mean-square (RMS) pressure coefficients for Case Ⅰ under 0° wind direction, while Figs. 6 and 7 exhibit the distributions of the mean pressure coefficients and RMS pressure coefficients for Case Ⅰ under 45°wind direction. From Figs. 4(a), 5(a), 6(a) and 7(a), it is observed that the formation of the separation bubble and conical vortex was not affected by the opening. On the other hand, the influences of the separation bubble and conical vortex on the internal pressures were realized when they entered into the interior space of the building model through the opening. As shown in Figs. 4(b), 5(b), 6(b) and 7(b), the existence of the separation bubble and conical vortex resulted in the fierce mean and RMS pressure coefficients in the internal volume of the building model. Meanwhile, due to the fact that the wind pressure propagation speed was equivalent to the speed of sound, the distributions of internal mean and RMS pressure coefficients were relatively uniform and only the pressure amplitudes near the orifice were disturbed by the orifice.

Through superposition of instantaneous internal and external pressures acquired synchronously, the time series of the net pressures on the roof are obtained. As exhibited in Figs. 4(c), 5(c), 6(c), and 7(c), the mean and RMS net pressure coefficients were different from the external mean and RMS pressure coefficients. But, the differences were mainly observed in the magnitudes of the coefficients. Compared with the mean external pressure coefficients, the mean net pressure coefficients in the region under the separated bubble and conical vortex decreased due to the offsetting effect of high internal suctions, while the RMS net pressure coefficients didn't weakened too much. Outside this region, the mean net pressure coefficients became positive, while the RMS net pressure coefficients were not diminished because of the superposition effect. It is noted that the RMS net pressure coefficients were larger than the external ones.

During strong windstorms such as typhoons, wind speed and direction may vary significantly (Li *et al*. 2012). This may make a corner-damaged roof of a low-rise building sometimes bear positive wind pressure and sometimes withstand suctions. This may cause destroy of the whole roof or fatigue damage of subsidiary components. It should be noted that the similar pressure distribution characteristics were also observed for other corner opening configurations in this study.

3.2 Correlative relationship of internal pressures

To understand the relevance of internal fluctuating pressures, five internal measuring taps (D29、

D56、D139、D164 and D214) were randomly selected in this study, whose locations are shown in Fig. 1. Tables 1 and 2 list the cross-correlation coefficients between the five selected points. The upper and lower triangles in Table 1 respectively stand for case Ⅰ and case Ⅲ for 0° wind direction. On the other hand, the upper and lower triangles in Table 2 delegate case Ⅳ and case Ⅴ for 45° wind direction, respectively. From the tables, it is found that the cross-correlation coefficients between the measuring points increased with the decrease of the opening area on the roof corner. The reason is that the smaller opening is closer to the windward roof corner and edges where the influence of the conical vortices is stronger and the higher suctions make the internal pressures more even. It is found that all the correlation coefficients are above 0.9, which indicates that the internal fluctuating wind pressures have high correlative relationship.

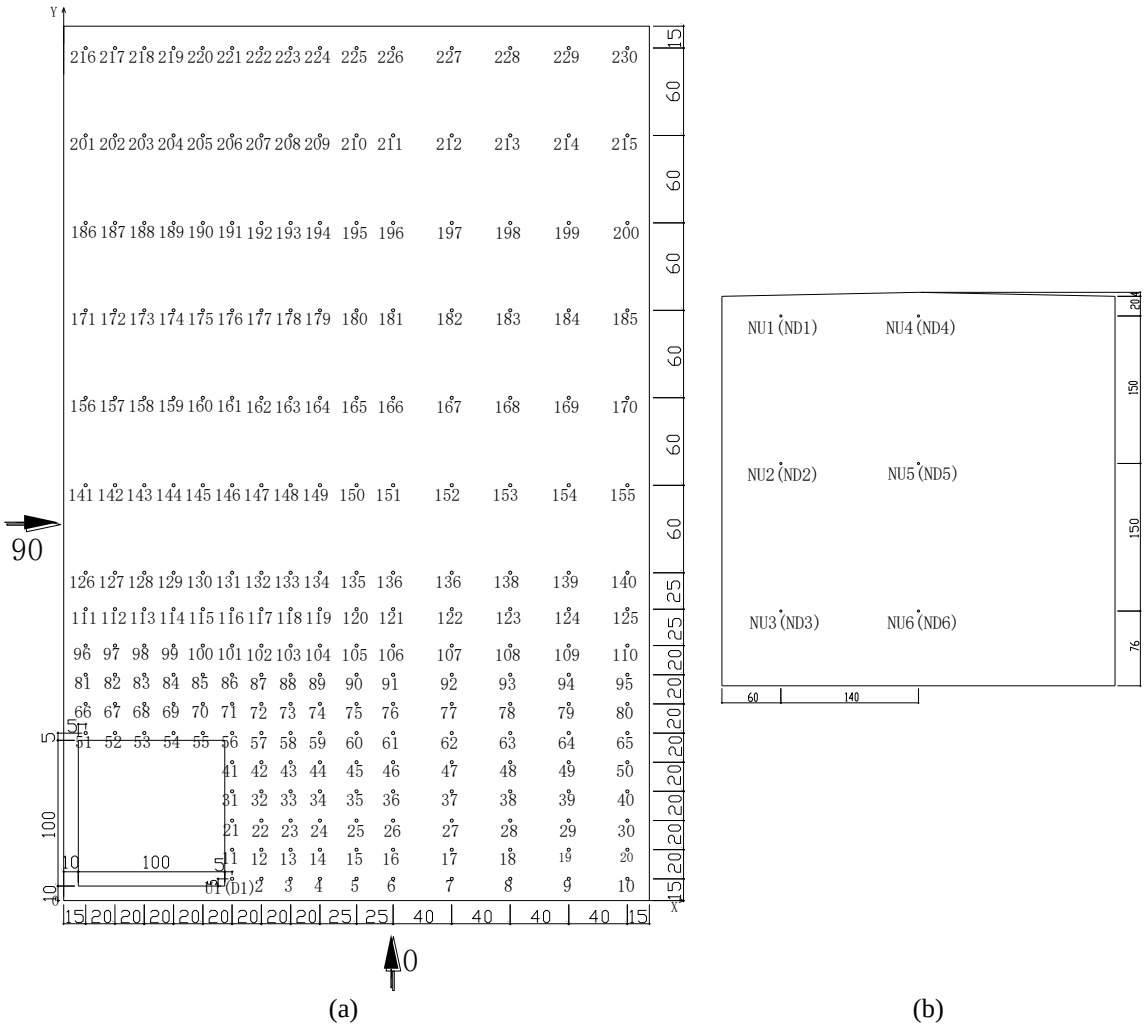

(a) (b)

Continued-

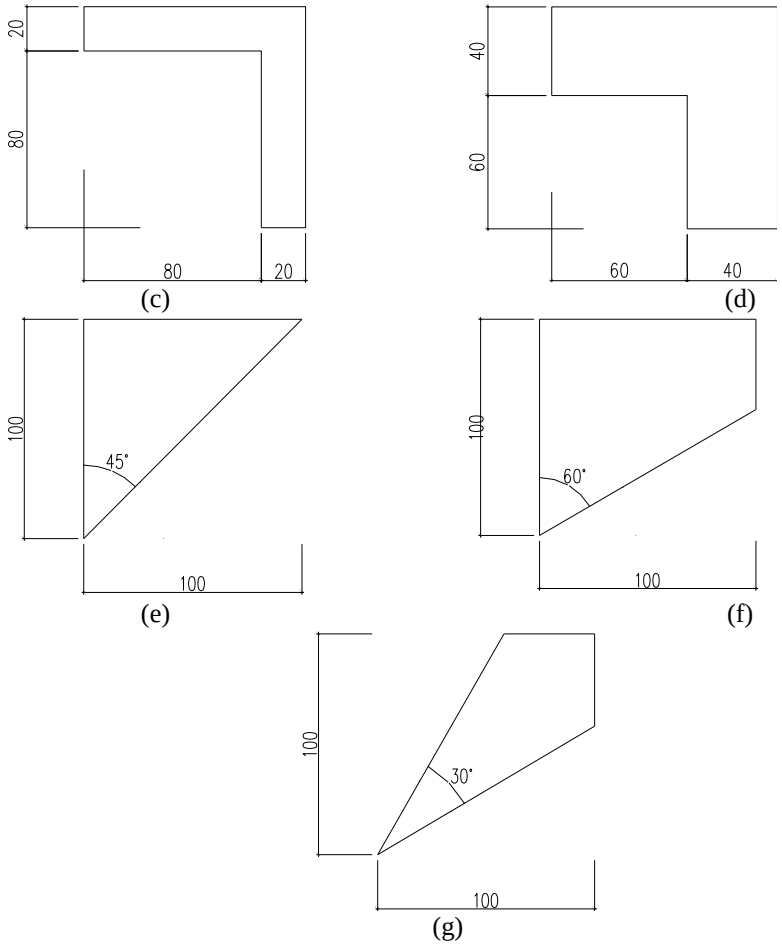

Fig. 1 Tap locations and definition of wind direction. (a) Roof taps (Case Ⅰ) (b) Wall taps (c) Case Ⅱ (d) Case Ⅲ (e) Case Ⅳ (f) Case Ⅴ (g) Case Ⅵ (unit：mm)

Table 1 Cross-correlation coefficients of internal fluctuating wind pressures under 0° wind direction (Case Ⅰ and Case Ⅲ)

Taps	D29	D56	D139	D164	D214
D29	1.00	0.95	0.94	0.95	0.94
D56	0.96	1.00	0.95	0.94	0.96
D139	0.94	0.95	1.00	0.94	0.95
D164	0.96	0.95	0.94	1.00	0.94
D214	0.95	0.96	0.94	0.95	1.00

Table 2 Cross-correlation coefficients of internal fluctuating wind pressures under 45° wind direction (Case Ⅳ and Case Ⅴ)

Taps	D29	D56	D139	D164	D214
D29	1.00	0.97	0.97	0.98	0.97
D56	0.98	1.00	0.97	0.97	0.98
D139	0.98	0.97	1.00	0.97	0.97
D164	0.99	0.98	0.98	1.00	0.97
D214	0.98	0.99	0.98	0.98	1.00

Fig. 2 Building model in the wind tunnel testing

Coherence functions between internal tap D29 near the edge of the opening and other four internal taps (D56、D139、D164 and D214) for all the cases under 0° and 45° wind directions are given in Figs. 8 and 9, respectively. According to the figures, the coherence function curves for the different cases under the same wind direction are almost identical. The coherence functions are close to 1 at frequency of 0 Hz, while in the range of 0 Hz to 8 Hz the coherence functions are all above 0.9, which demonstrates that the internal pressures have a good coherent relationship in frequency domain. Contrasting the coherence functions under different wind directions, it is found that the curves of the coherence functions are not alike, which attributes to different influencing mechanisms. For example, under 0° wind direction, the separation bubble has a significant effect on the coherence functions, while the conical vortices play an important role for those under 45° wind direction. No matter for 0° or 45° wind direction, the coherence function for the mono-triangle-opening case Ⅴ is larger than that for the bi-triangle-opening case Ⅵ in the range of 0 Hz to 30 Hz. Generally speaking, the stronger the conical vortex, the more violent the suctions, and also the greater of the correlation of the pressures under the conical vortex are. From the points of the foregoing phenomenon and view, it can be concluded that the effect of a single

conical vortex on the internal pressures contains much more low-frequency energy than that of a paired conical vortex.

In general, coherence function of pressures at different locations has a trend of continuous attenuation with the increasing of frequency (Matsumoto *et al*. 2003). As revealed in Figs. 8 and 9, however, there appear two clear peaks on the curves of the coherence functions. One is around 35 Hz, and the other is near 42 Hz, where the values of the coherence functions are greater than 0.8.

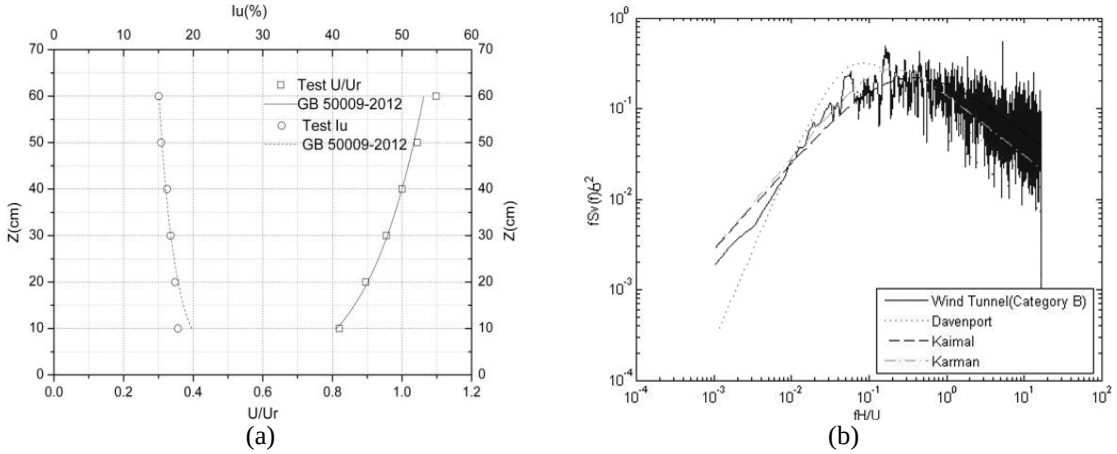

(a) (b)

Fig. 3 Atmospheric boundary layer simulated in the wind tunnel, (a) Mean longitudinal wind speed and turbulence intensity profiles (b) Spectra of longitudinal wind speed

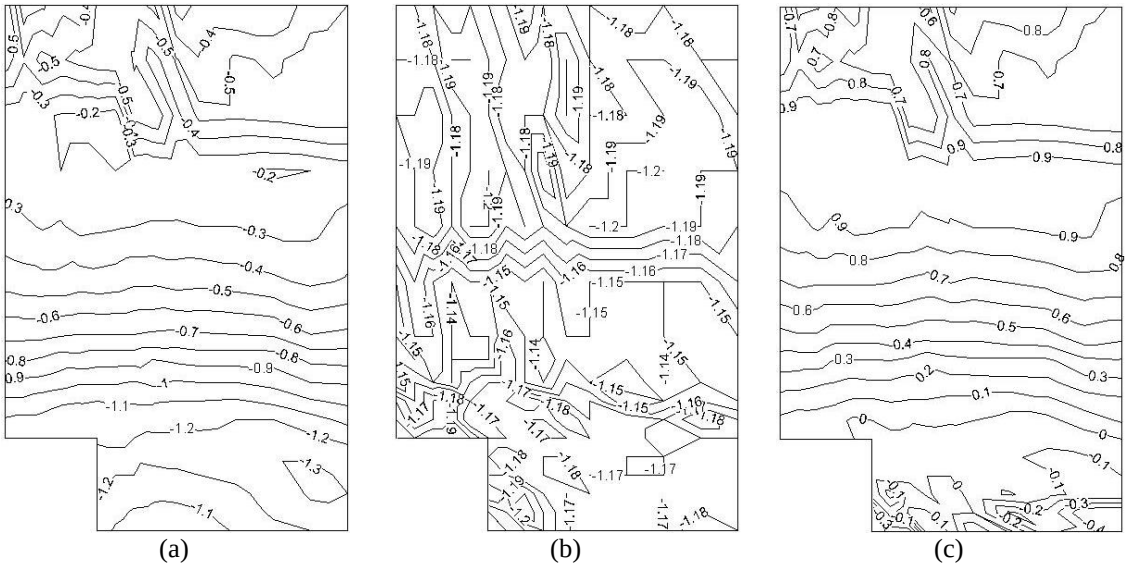

(a) (b) (c)

Fig. 4 Distributions of mean pressure coefficients on the roof under 0° wind direction, mean external pressure coefficients (b) mean internal pressure coefficients (c) mean net pressure coefficients

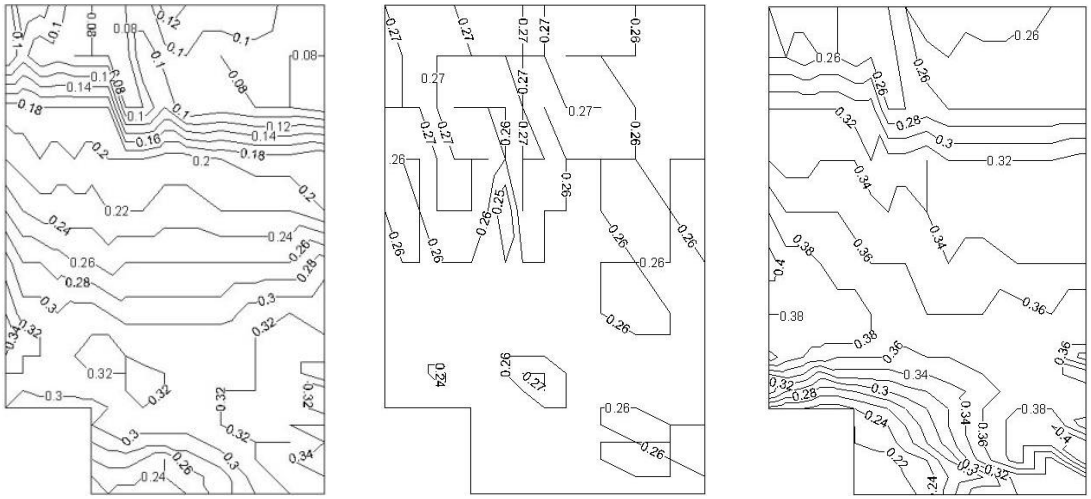

(a) (b) (c)

Fig. 5 Distributions of RMS pressure coefficients on the roof under 0° wind direction, RMS external pressure coefficients (b) RMS internal pressure coefficients (c) RMS net pressure coefficients

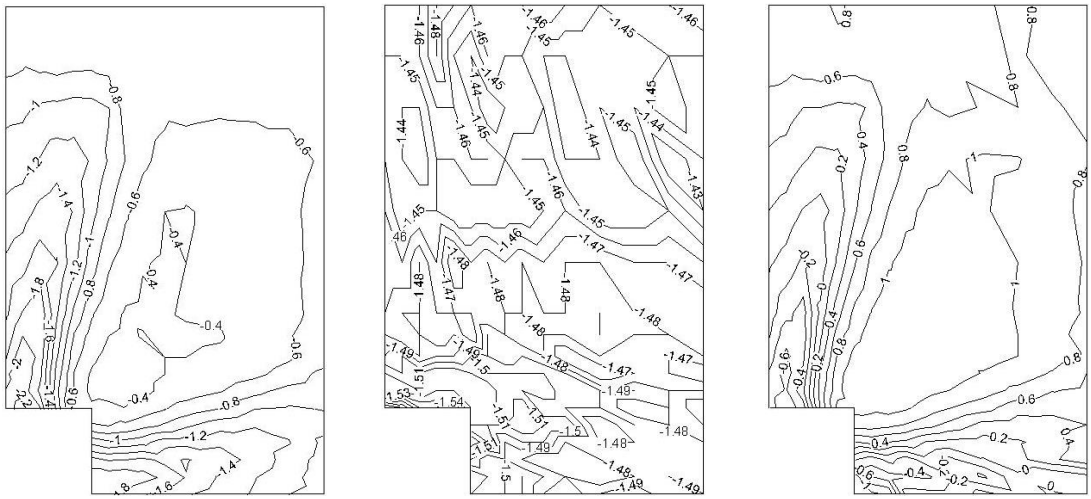

(a) (b) (c)

Fig. 6 Distributions of mean pressure coefficients on the roof under 45° wind direction, (a) mean external pressure coefficients (b) mean internal pressure coefficients (c) mean net pressure coefficients

This illustrates high correlation of internal fluctuating pressures at these two frequencies. The peaks at the two frequencies were caused by different revulsive mechanisms. Considering the influence factors of the internal pressures, it is inferred that one peak of the coherence functions is caused by the characteristic turbulences (separation bubble or conical cortex), and the other peak is induced by the opening at the roof corner and the internal volume.

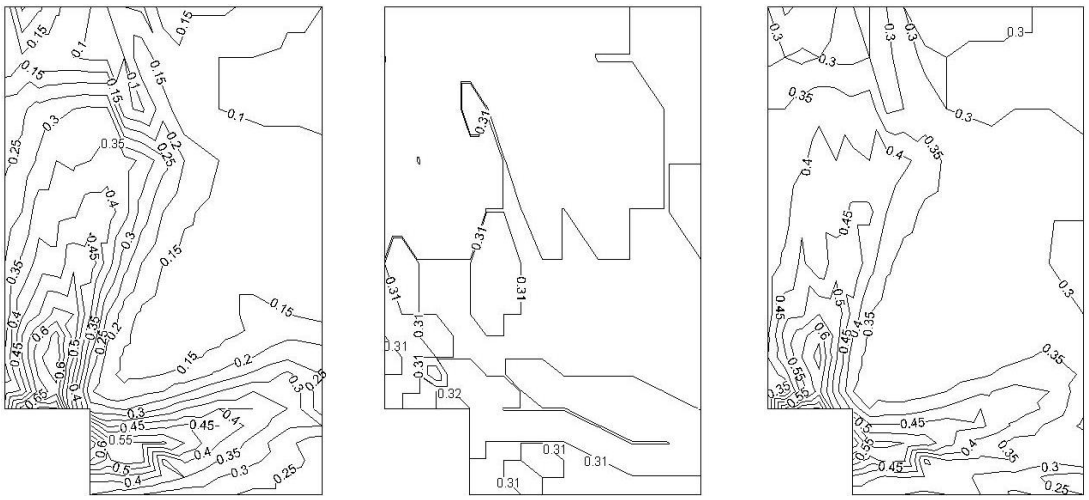

(a) (b) (c)

Fig. 7 Distributions of RMS pressure coefficients on the roof under 45° wind direction, (a) RMS external pressure coefficients (b) RMS internal pressure coefficients (c) RMS net pressure coefficients

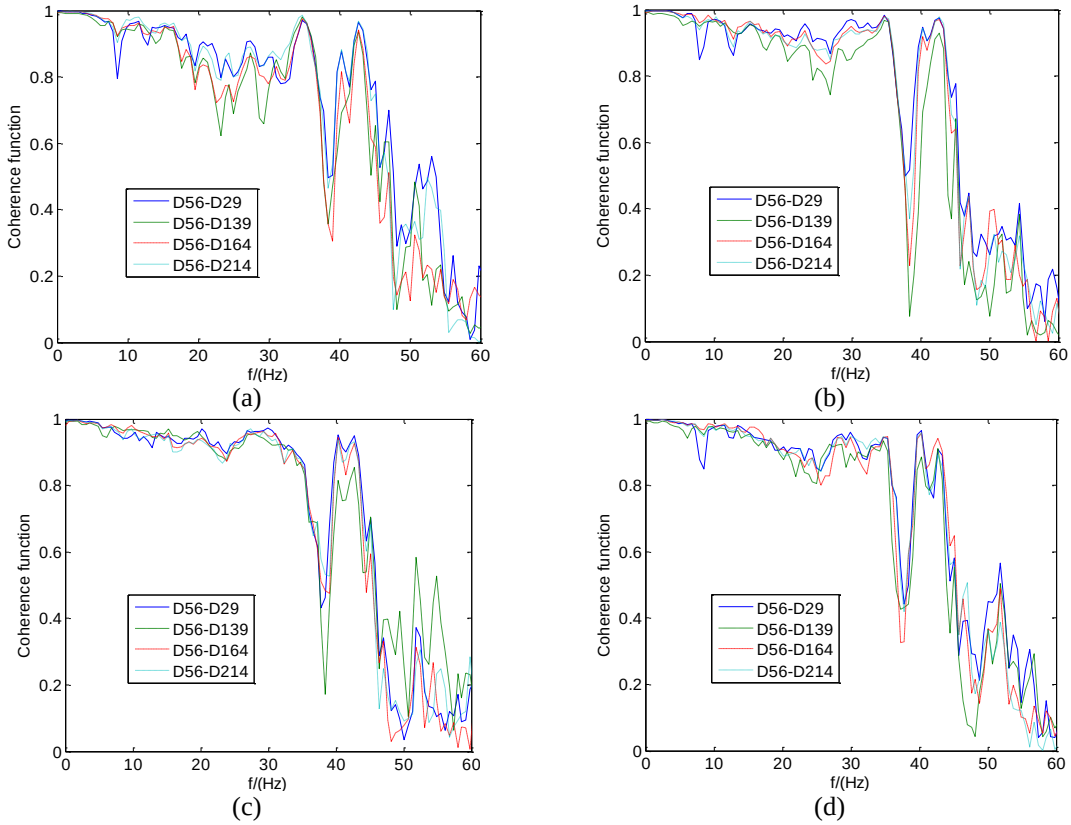

(a) (b) (c) (d)

Continued-

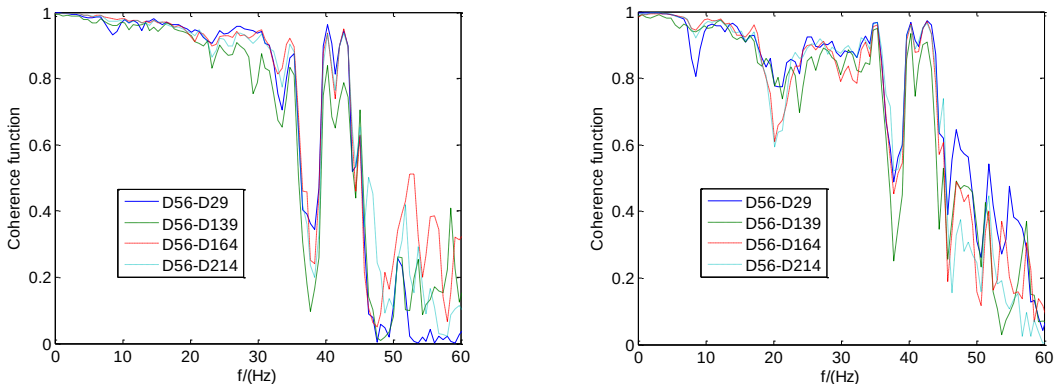

Fig. 8 Coherence functions of internal pressures under 0° wind direction, (a) Case I (b) Case II (c) Case III (d) Case IV (e) Case V (f) Case VI

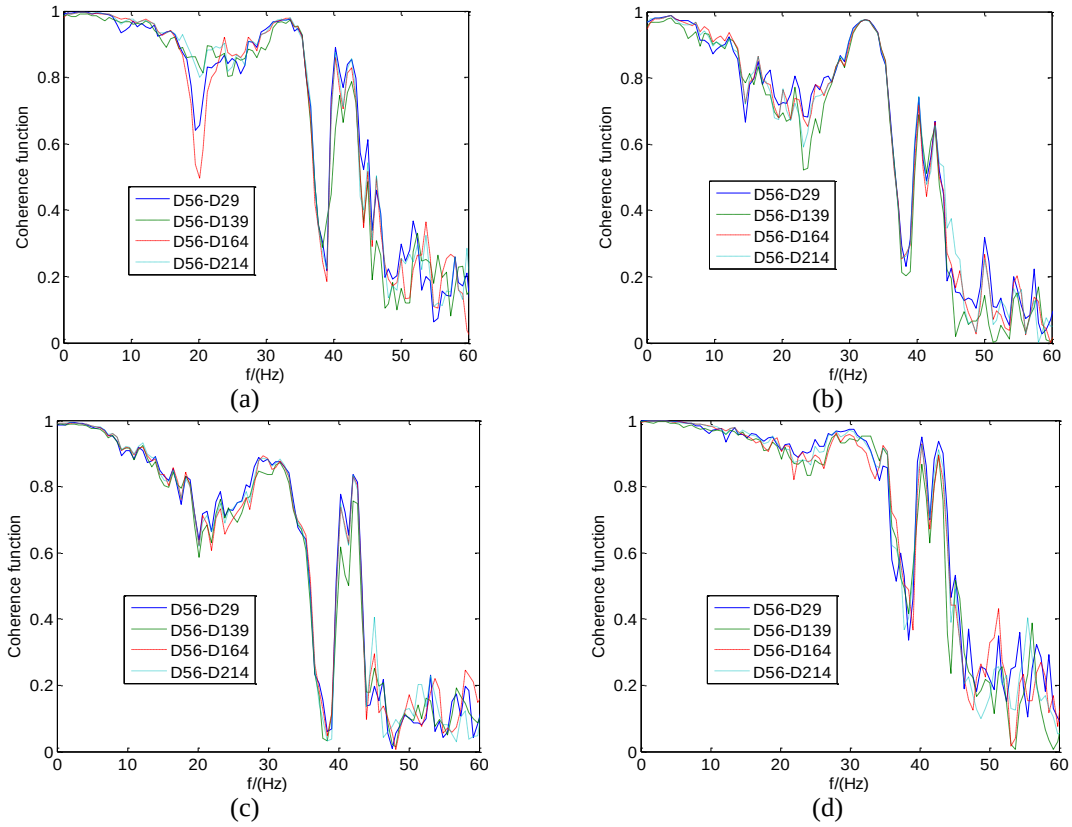

Continued-

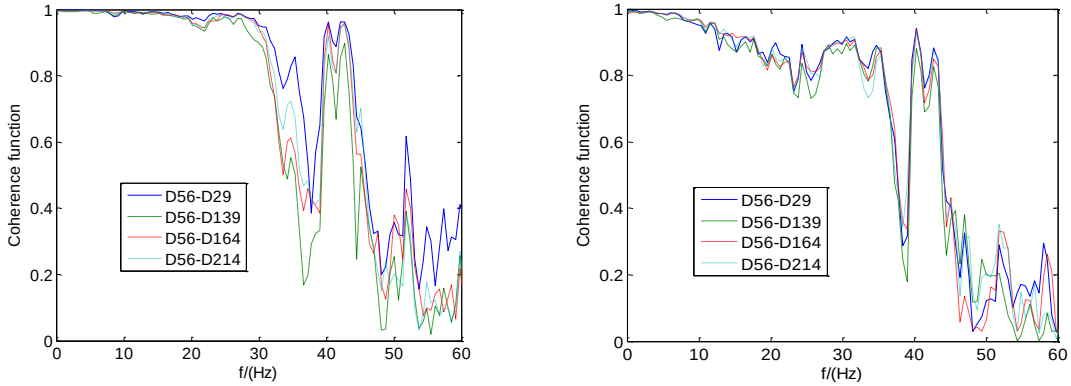

Fig. 9 Coherence functions of internal pressures under 45° wind direction, (a) Case Ⅰ (b) Case Ⅱ (c) Case Ⅲ (d) Case Ⅳ (e) Case Ⅴ (f) Case Ⅵ

3.3 Correlation between internal and external pressures

Not only separation bubble and conical vortex give rise to the internal fluctuating pressures through the openings on the roof corner, but they also influence the distributions of the external pressures on the roof. Hence, the correlation between the internal and external pressures is worth of investigation. Figs. 10 and 11 show the distributions of the correlation coefficients between the internal and external fluctuating pressures under 0° and 45° wind direction, respectively. For 0° wind direction, the distributions of the correlation coefficients for all the cases are semblable, while the values are relatively large near the openings and the largest values are even above 0.8. With the increase of the distance to the orifice edge, the correlation coefficients decrease and in some areas even negative values are observed.

Broadly speaking, in the wind tunnel study, the effect of the size of the rectangular opening on the correlation coefficients between the internal and external pressures under 0° wind direction is not significant. The correlation coefficients only weakly decrease with the increase of the rectangular orifice areas. The triangle orifice areas have the same effect on the correlation coefficients. Comparing the correlation coefficients of the rectangular-opening cases with those of the triangle-opening cases under 0° wind direction, we can easily find that the correlation coefficients of the rectangular-opening cases are a little larger than those of the triangle-opening cases. Moreover, the correlation coefficients of the mono-triangle-opening cases are less than those of the bi-triangle-opening cases.

It can be seen from Fig. 11 that, under 45° wind direction, the correlation coefficients of the internal and external pressures have a similar distribution pattern with the external mean pressure coefficients, exhibiting cone-shape distributions along the windward edge on the roof. The correlation coefficients decrease from the windward corner to the downstream zones. The largest coefficient is found in the windward corner vortex core region, which comes to more than 0.85. Beyond the region of the conical vortex, the correlation coefficients are small and uniform, at about 0.2. For the oblique incident flows, the effects of the sizes of the rectangular openings on the correlation coefficients are not significant.

And notably, for the single-triangle-opening cases under 45° wind direction, the distributions of

the correlation coefficients between the internal and external pressures present four ribbon-shape zones. The first one is the zone with strong correlation coefficients along the short windward edge, followed by the zone with relatively weak values, the next is the zone with relatively strong correlation coefficients, and the final is the zone with weak values along the long windward edge. However, for the bi-triangle-opening case Ⅵ, the correlation coefficient distribution is similar to those of the cases of rectangular openings, which reveals that the phenomenon of the ribbon-shape distribution will turn up on the condition that only one conical vortex affects the internal pressures.

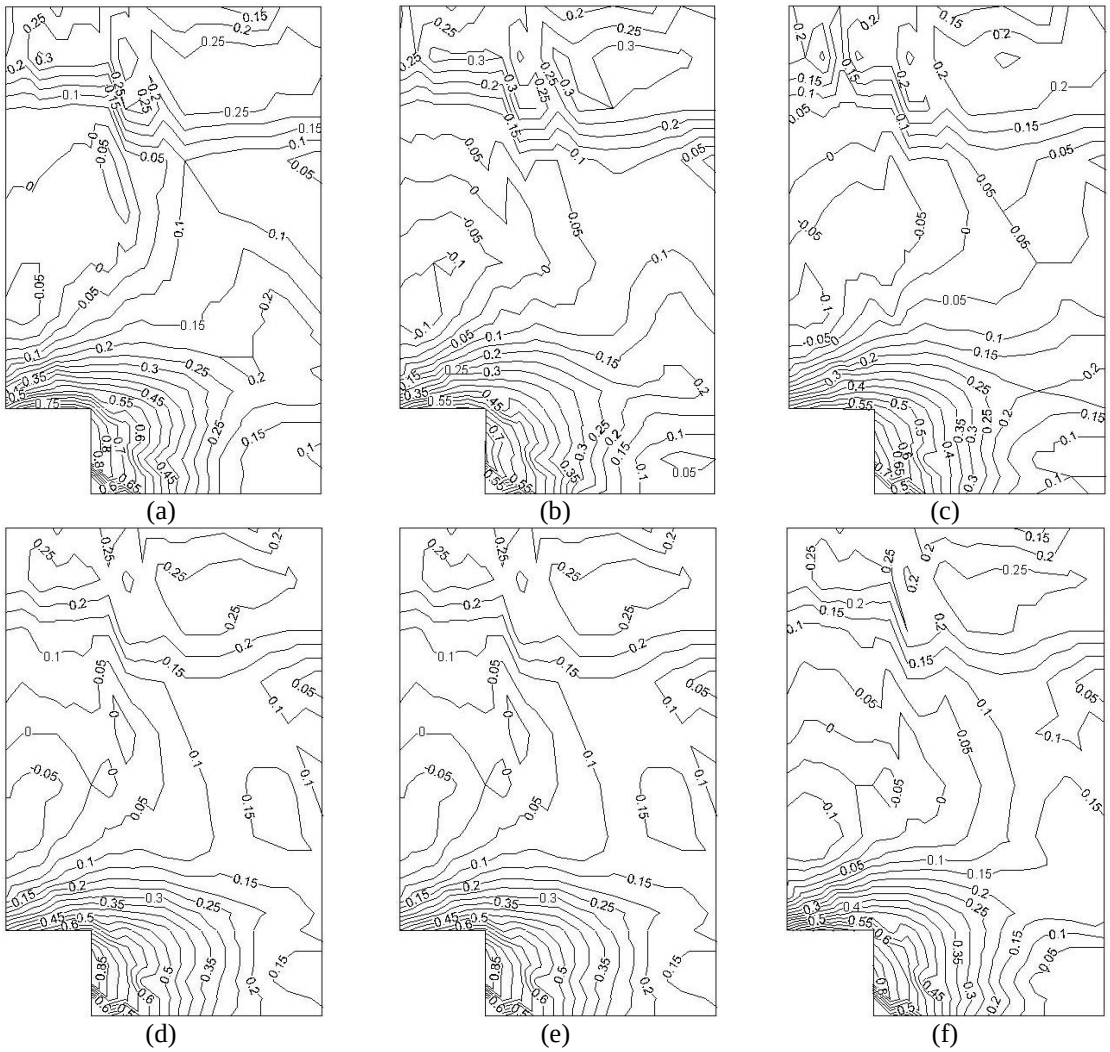

Fig. 10 Correlation coefficients between external and internal pressures of the roof under 0° wind direction. (a) Case Ⅰ (b) Case Ⅱ (c) Case Ⅲ (d) Case Ⅳ (e) Case Ⅴ (f) Case Ⅵ

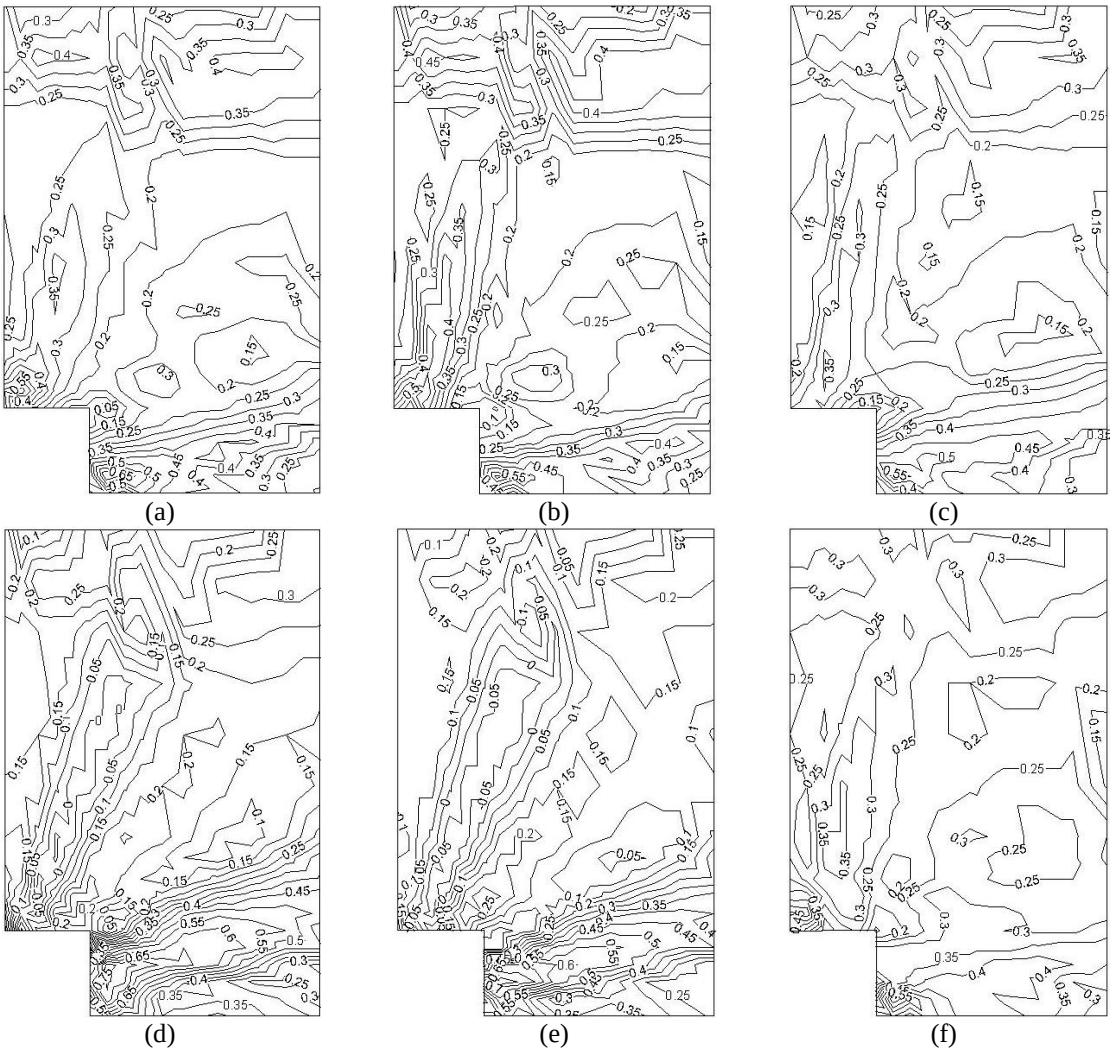

Fig. 11 Correlation coefficients between external and internal pressures of the roof under 45° wind direction. (a) Case Ⅰ (b) Case Ⅱ (c) Case Ⅲ (d) Case Ⅳ (e) Case Ⅴ (f) Case Ⅵ

3.4 Internal area-weighted pressure coefficients

From the above analysis, it was observed that the internal pressures of a house with an opening at a roof corner show a characteristic of overall synchronization. Therefore, we may use a uniform variable to describe the internal pressures. Here we illustrate the issue with the area-weighted pressure coefficient, which is defined in the following equation.

$$Cp(t) = \frac{\sum_{i=1}^{n} Cp_i(t)A_i}{\sum_{i=1}^{n} A_i} \tag{4}$$

where, $C_p(t)$ represents the time series of the internal area-weighted pressure coefficient, $C_{pi}(t)$ and A_i are the pressure coefficient and affiliated area at tap i, respectively. Fig. 12 shows the variations of the statistics of the internal area-weighted pressure coefficients with wind direction. As the change of the wind direction, the variation of the average and minimum pressure coefficients for the case of square openings (holes) is roughly 'W' shape and that of the RMS pressure coefficients is 'M' type. The curve of the average pressure coefficient is relatively smooth, while the root-mean-square and minimum pressure coefficients change violently. With the decrease of the opening area, the amplitudes of the wind pressure coefficients have an increasing trend. It is interesting to note that, taking 45° wind direction as the axis of symmetry, the wind pressure coefficients do not follow completely symmetric distributions. Compared with the pressure coefficients under larger wind directions, the amplitudes of the pressure coefficient under smaller wind directions are much larger. This shows that conical vortices along the longer edge are much stronger than that along the shorter side for the symmetry axis of 45° wind direction. This is because the longer front edges contribute a longer distance for the development of conical vortices, which cause stronger suctions on the roof.

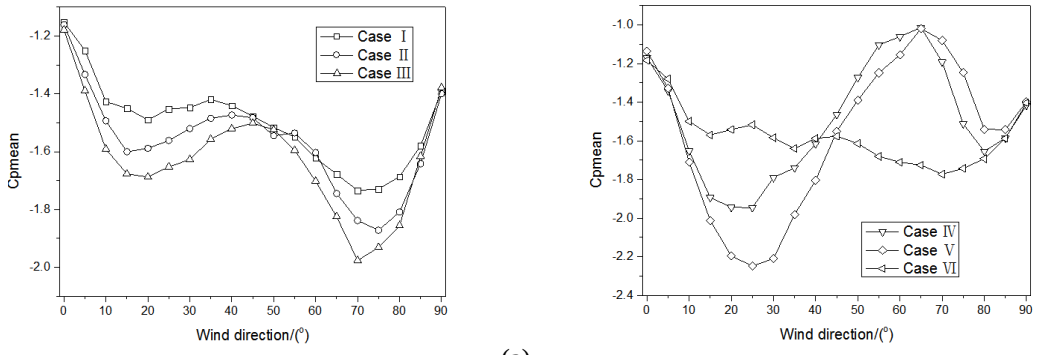

(a)

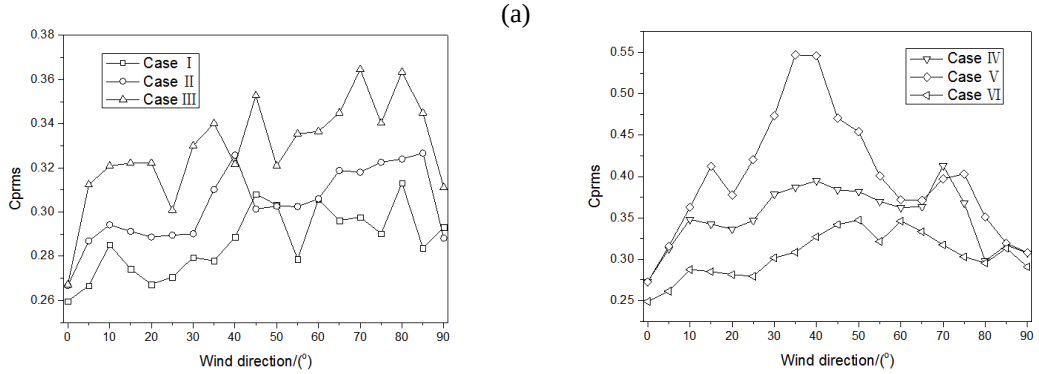

(b)

Continued-

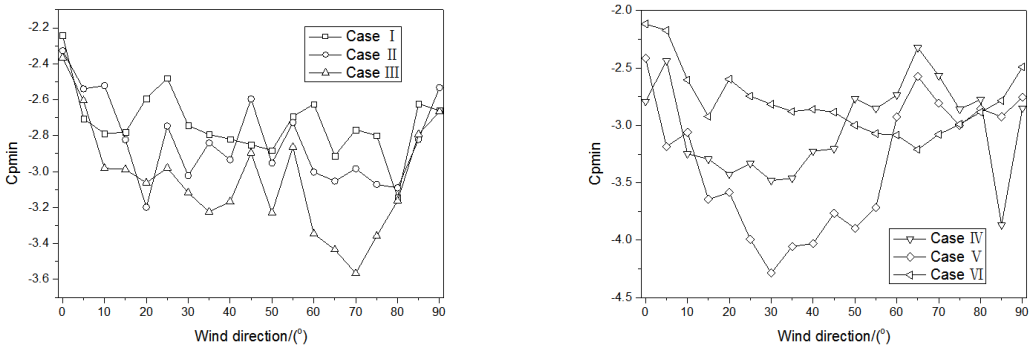

(c)

Fig. 12 Vatiations of area-weighted internalpressure coefficientswith wind direction, mean pressure coefficients (b) RMS pressure coefficients (c) minimun pressure coefficients

For a single triangle opening, the curve of the average wind pressure coefficient is with an inverted 'S' shape, and the amplitudes increase first, then decrease and increase afterwards. The general trend of the amplitudes of the RMS and minimum pressure coefficients increases first and then decreases. But, the variations are significantly dependent on the wind directions. With the decrease of the opening area, the amplitudes of the statistics for each wind direction have an increasing trend. This is because a smaller opening is closer to the front edge and windward roof corner, where the conical vortex and separation bubble are stronger. It is worth mentioning that, unlike the case Ⅴ, the amplitudes of the pressure coefficients for case Ⅵ do not vary significantly with the wind direction. This shows that the double triangle openings are much less destructive than a single opening. On the other hand, it demonstrates that the effect of conical vortex in pair on the internal pressure is not stronger than that of a unilateral conical vortex. This also illustrates that conical vortex along the two front sides do not get stronger or weaker simultaneously. That is to say, the intensity variation between them is not simultaneous. Comparing the square opening cases with the triangle opening cases, it is noted that the amplitudes of the pressure coefficients for a triangle case under the most unfavorable wind direction are much greater, which may result in more serious damage consequences.

3.5 Influence of the internal pressures on the net pressures on the roof

In order to analyze the effect of the internal pressures on the net pressures on the roof, we select the most unfavorable situation: case Ⅴ under 30° wind angle, with contrasting changes of the internal, external and net pressure coefficients for taps perpendicular to the windward edge, as shown in Table 3. Under the most adverse circumstance, all the net pressure coefficients are positive. Comparing with the external root-mean-square pressure coefficients, only a small portion of the fluctuating net pressure coefficients decrease because of the superimposition with the internal pressures. This change is related to the correlation between the internal and external pressures. The larger the correlation coefficients, the smaller the standard deviations of the net pressure coefficients are. Taps with larger correlation coefficients are within the scope of the conical vortices, especially in the vortex core zones.

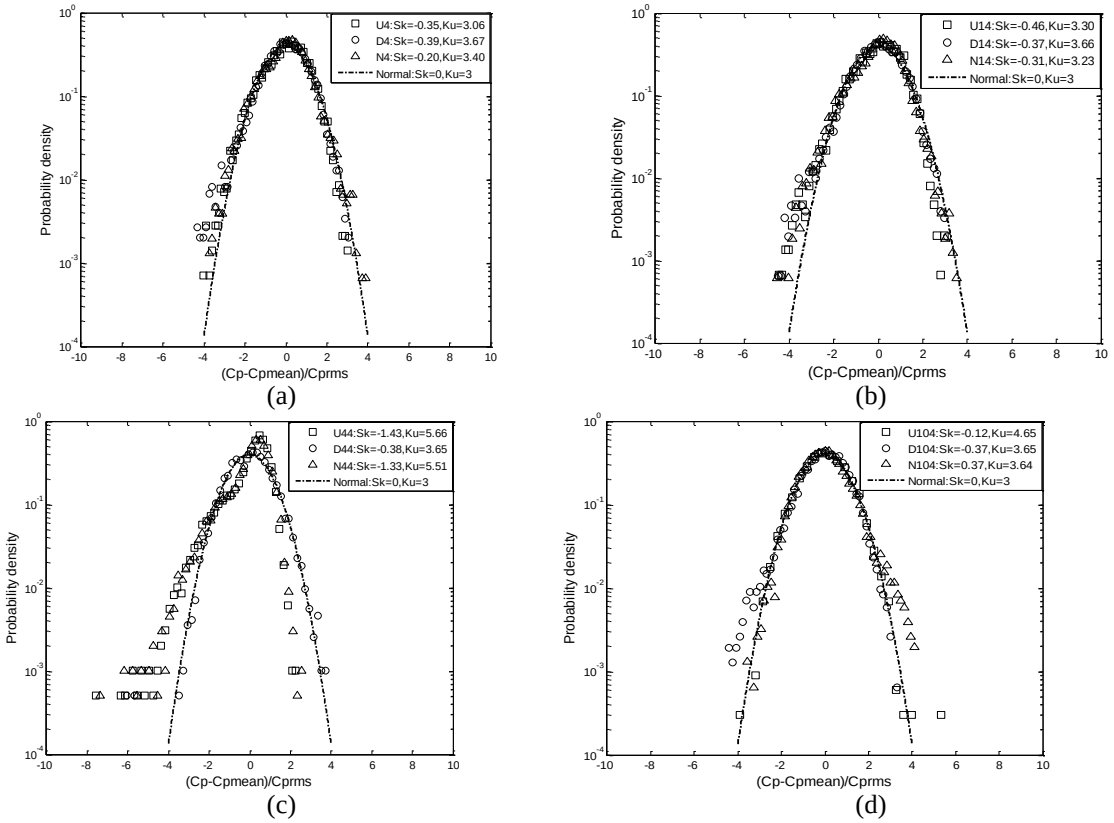

Fig. 13 Probability density functions of pressure coefficients, (a) Tap 4; (b) Tap 14; (c) Tap 44; (d) Tap 104

Table 3 Internal, external and net pressure coefficients for Case Ⅴ under 30° wind direction

Taps	C_{pdmean}	C_{pumean}	C_{pnmean}	C_{pdrms}	C_{purms}	C_{pnrms}	ρ_{nd}
4	-2.25	-1.82	0.43	0.58	0.35	0.57	0.33
14	-2.23	-2.12	0.11	0.57	0.46	0.60	0.34
24	-2.24	-1.98	0.26	0.56	0.56	0.43	0.77
34	-2.26	-1.15	1.11	0.57	0.64	0.48	0.68
44	-2.26	-0.67	1.59	0.57	0.43	0.53	0.47
59	-2.25	-0.47	1.78	0.57	0.22	0.57	0.20
74	-2.24	-0.41	1.83	0.57	0.15	0.58	0.01
89	-2.26	-0.43	1.83	0.57	0.13	0.59	-0.01
104	-2.25	-0.43	1.82	0.58	0.11	0.59	0.04

Note: C_{pdmean}, C_{pumean} and C_{pnmean} are the internal, external and net mean pressure coefficients, respectively., C_{pdrms}, C_{purms} and C_{pnrms} are the internal, external and net RMS pressure coefficients, respectively; ρ_{nd} is the correlation coefficient

Figs.13(a)-13(d) exhibit the probability density functions of the internal, external and net pressure coefficients for tap 4 in windward edge zone, tap 14 in vortex core zone, tap 44 in vortex reattachment zone and tap 104 in vortex shedding zone, respectively. The probability density functions of the internal pressure coefficients are close to the Gaussian distribution, and the values of skewness and kurtosis do not appear to be much different from those of the Gaussian distribution. The degrees that the external pressure coefficients deviate from the Gaussian distribution are associated with the locations of the measuring points. Vortex reattachment zone presents the biggest deviation extent. Due to the influence of the internal pressures, the probability density functions of the net pressures are less non-Gaussian compared with those of the external pressures. This is due to the fact that the standard deviations of the net pressures are smaller than those of the external pressures in conical vortex zones.

3.6 Shape factor of wind loading on the windward wall

The Chinese load code gives some specifications about the external and internal shape factors of wind loading for sealed buildings or buildings with a dominant opening on windward wall. Nevertheless, the load code does not consider the case that there is an opening on a roof corner. Hence, in order to study the external, internal and net shape factors on the windward wall when an opening is on the roof corner, wind pressure coefficients are converted into shape factor according to the definition of the shape factor in the load code. The conversion formula is as follows

$$\mu_s = \frac{Cpmean}{\left(\frac{z}{H}\right)^{0.3}} \tag{5}$$

where, μ_s represents the shape factor, C_{pmean} is the mean pressure coefficient, z is the height of the pressure tap, H is the reference height.

Fig. 14 shows the variations of the external, internal and net shape factors at different locations with the approaching wind direction for case Ⅰ. The external shape factors change from positive to negative with the increase of wind angles, and the variation ranges are different due to different locations of the pressure taps. Local shape factors of windward wall and sideward wall, stipulated in the load code, are 1.0 and -1.4, respectively. Considering the average effect on the values stipulated in the load code, the measured results for 0° and 45° wind directions are near to the specified values. The internal shape factors are all negative and the absolute values are greater than 1.0. Internal taps at the same height have almost the same values of the shape factors. With the decrease of the height, the amplitudes of the internal shape factors increase instead, which results from the uniform internal pressure coefficients. For a sealed building, the shape factors specified by the load code takes -0.2 or 0.2 depending on the pressures on the outside wall, which is far less than the experimental results on the condition that there is an opening on the roof corner. On account of large external positive shape factors and strong internal negative shape factors, the net shape factors on the windward wall are very large and the largest values even come to about 3.5. What is more, the largest net shape factor does not turn up under 0° wind direction, but occurs under near 20° wind direction. For 90° wind direction, the net shape factors are close to zero due to the offset effect of the internal and external suctions.

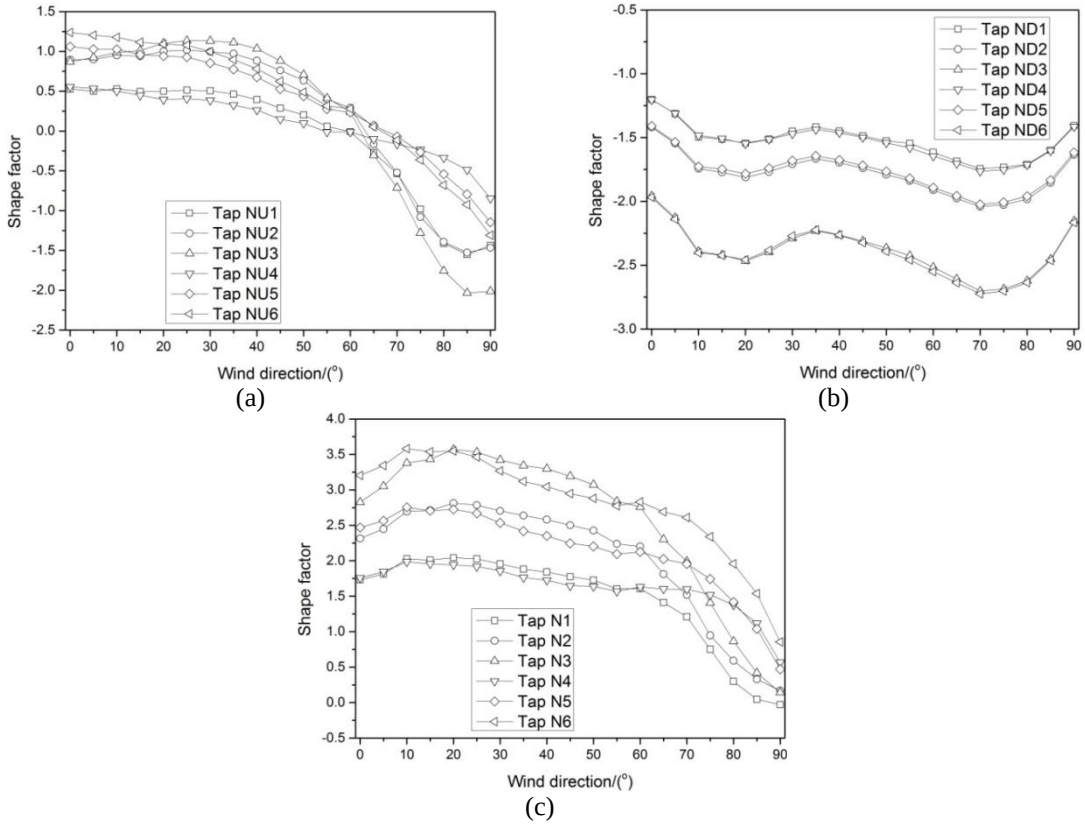

Fig. 14 Variations of shape factors of the windward wall with approaching wind directions, (a) external shape factors (b) internal shape factors (c) net shape factors

3.7 Frequency-domain characteristics

Fig. 15 shows the spectral densities of internal pressures at four inside measuring points for two situations. The power spectral densities almost completely overlap, which demonstrates that the internal fluctuating pressures also have a strong correlation in frequency domain. Taking no account of glitches in the high frequency range induced by fan impeller rotations and noises in the wind tunnel testing, there are two distinct spectral peaks, one near 35.1Hz and the other about 42.7 Hz.

To explain the cause of the above mentioned phenomenon, Fig. 16 presents the power spectra of the internal, external and net fluctuating pressure coefficients at tap 111 (see Fig. 1 for its location) for case Ⅰ under 45° wind direction. There appears a spectral peak for the external pressures in the high frequency range (about 42.7 Hz), which is the dominant vortex shedding frequency (hereinafter referred as vortex shedding frequency) under oblique wind directions. As the same as shown in Fig. 15, there are also two spectral peaks for the internal pressures, and one

is located at the vortex shedding frequency and the other is at the Helmholtz resonant frequency (hereinafter referred as Helmholtz frequency) caused by the opening (hole) on the roof corner. In all the cases, the Helmholtz frequencies are smaller than the vortex shedding frequencies. But, the spectral densities at the Helmholtz frequencies are greater than those at the vortex shedding frequencies, illustrating that the energies corresponding to the Helmholtz frequencies are much stronger.

The spectral density of the net pressure is shown in Fig. 16(c) and only one spectral pump appears at the Helmholtz frequency. The spectral pump at the vortex shedding frequency disappears because of the strong correlation between the internal pressure and external pressure in the conical vortex zone and the superimposition offset the effect of the vortex. By the same token, without the occurrence of the Helmholtz resonance on the external pressures, the spectral peak of the net pressure at the Helmholtz frequency is not vanished.

Table 4 provides the Helmholtz frequencies for case Ⅰ under different wind directions. All the Helmholtz frequencies are almost identical, from which we can deduce that the wind direction has no effect on the Helmholtz frequencies.

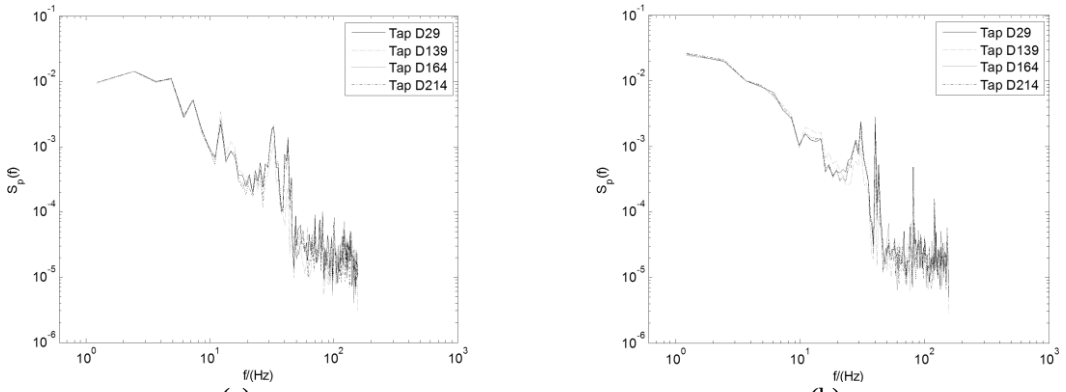

Fig. 15 Spectra of internal pressures. (a) Case Ⅰ under 0° wind direction (b) Case Ⅳ under 45° wind direction

Table 4 Helmholtz frequencies of case Ⅰ under different wind directions

Wind direction	0°	5°	10°	15°	20°	25°	30°	35°	40°	45°
Helmholtz frequency (Hz)	35.08	35.10	35.00	35.11	35.13	35.08	35.06	35.10	35.02	35.11

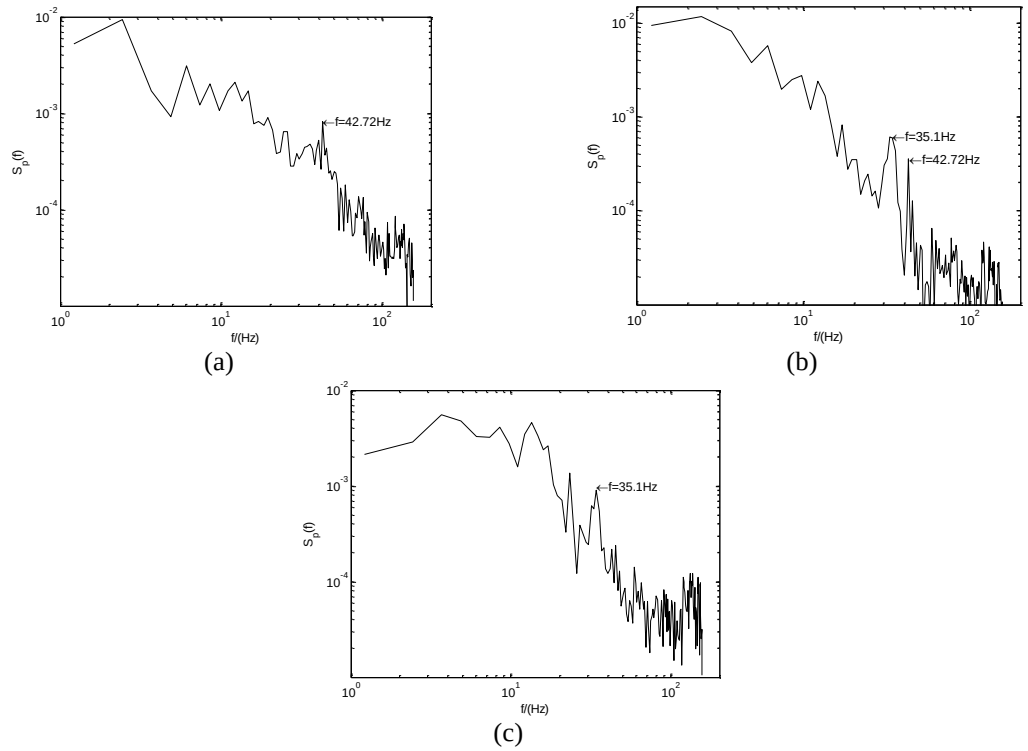

Fig. 16 Pressure spectra for tap 111 for case Ⅰ under 45° wind direction, (a) spectra of external pressure (b)spectra of internal pressure (c) spectra of net pressure

4. Conclusions

In this paper, through the simulation of roof corner damages by openings (holes) on a roof corner of a low-rise building, wind tunnel testing and subsequent analysis of the testing data were conducted to investigate the characteristics of internal, external and net pressures for the roof with openings of different sizes and shapes.

- Openings on the roof corner did not affect the formation of the separation bubble and conical vortex. Meanwhile, the separation bubble and conical vortex passed into the internal cavity and led to relatively uniform internal suction.
- The internal pressures show a good correlative relationship in both time and frequency domain. Therefore, a uniform variable can be used to describe the internal pressures.
- The effect of the size of the rectangular and bi-triangle openings on the correlation coefficients between the internal and external pressures is not significant. For the distributions of the correlation coefficients between the internal and external pressures under oblique wind directions, only the single-triangle-opening case presents four ribbon-shape zones.
- Superimposition of the internal and external pressures made the occurrence of positive net pressures on some areas of the roof. The probability densities of the internal pressures are close to the Gaussian distribution. Due to the offset effect of the internal pressures, non-Gaussian

characteristic of the net pressure is less profound compared with that of the external pressures.

- Affected by the effects of both Helmholtz resonance and vortex shedding, the spectrum of the internal pressures has two spectral peaks at the Helmholtz frequency and the vortex shedding frequency, respectively. However, the spectral peak of the net pressures at the vortex shedding frequency is counteracted. Moreover, the wind direction has no effect on the Helmholtz frequencies.
- Characteristics of the internal pressures can indirectly reflect some features of the conical vortex, such as the length of the leading edge is conductive to the development of the conical vortex, making the conical vortex much stronger.

Acknowledgements

The work described in this paper was fully supported by the "985" Project of Hunan University and grants from National Natural Science Foundation of China Project (No:51478405) and the Research Committee of City University of Hong Kong (Project No: 7004172).

References

Blocken, B. and Persoon, J. (2009), "Pedestrian wind comfort around a large football stadium in an urban environment: CFD simulation, validation and application of the new Dutch wind nuisance standard", *J. Wind Eng. Ind. Aerod.*, **97**(5-6), 255-270.

GB50009-2012 (2012), Load code for the design of building structures, China Architecture & Building Press, Beijing.

Ginger, J.D., Mehta, K.C. and Yeatts, B.B. (1997), "Internal pressures in a low-rise full-scale building", *J. Wind Eng. Ind. Aerod.*, **72**, 163-174.

Guha, T.K., Sharma, R.N. and Richards, P.J. (2011), "Internal pressure dynamics of a leaky building with a dominant opening", *J. Wind Eng. Ind. Aerod.*, **99**(11), 1151-1161.

Holmes, J.D. and Ginger, J.D. (2012), "Internal pressures – The dominant windward opening case – A review", *J. Wind Eng. Ind. Aerod.*, **100**(1), 70-76.

Holmes, J.D. (1979), "Mean and fluctuating internal pressures induced by wind", *Proceedings of the 5th Int. Conf. Wind Eng.*.

Huang, P. and Gu, M. (2004), "Experimental study and comparison analysis on wind load of a large span cantilever roof ", *J. Struct. Eng.- ASCE*, **20**(4), 51-55.

Kawai, H. (2002), "Local peak pressure and conical vortex on building", *J. Wind Eng. Ind. Aerod.*, **90**(4-5), 251-263.

Kopp, G.A. and Morrison, M.J. (2012), "Full-scale testing of low-rise, residential buildings with realistic wind loads", *J. Wind Eng. Ind. Aerod.*, **104-106**, 25-39.

Li, Q.S., Dai, Y.M. and Li, Z.N. (2010), "Wind pressures on low-rise building surface during a severe typhoon 'Hagupit'", *J. Build.Struct.*, **31**(4), 62-68.

Li, Q.S., Hu, S.Y., Dai Y.M. and Li Z.N. (2010), "Analysis of the field measured suction peak pressure coefficients on a flat roof of a low-rise building", *J. Hunan Univ.*, **37**(6), 11-16.

Li, Q.S., Hu, S.Y., Dai, Y.M. and He, Y.C. (2012), "Field measurements of extreme pressures on a flat roof of a low-rise building during typhoons", *J. Wind Eng. Ind. Aerod.*, **111**(12), 14-29.

Liu, H. and Saathoff, P.J. (1981), "Building internal pressure: sudden change", *J. Eng. Mech. Div.*, **107**(2), 309-321.

Mahmood, M. (2011), "Experiments to study turbulence and flow past a low-rise building at oblique

incidence", *J. Wind Eng. Ind. Aerod.*, **99**(5), 560-572.
Matsumoto, M., Shirato, H., Aaraki, K., Haramura, T. and Hashimoto, T. (2003), "Spanwise coherence characteristic of surface pressure field on 2D bluff bodies", *J. Wind Eng. Ind. Aerod.*, **91**(1-2), 155-163.
Pan, F., Cai, C.S. and Zhang, W. (2013), "Wind-induced internal pressures of buildings with multiple openings", *J. Eng. Mech - ASCE.*, **139**, 376-385.
Sharma, R.N. (2013), "Internal and net proof pressures for a dynamically flexible building with a dominant wall opening", *Wind Struct.*, **16**(1), 93-115.
Sharma, R.N. and Richards, P.J. (2003), "The influence of Helmholtz resonance on internal pressures in a low-rise building", *J. Wind Eng. Ind. Aerod.*, **91**(6), 807-828
Stathopoulos, T. and Luchian, H.D. (1989), "Transient wind-induced internal pressure", *J Eng. Mech.- ASCE*, **115**(7), 1501-1513.
Tecle, A.S., Bitsuamlak, G.T. and Aly, A.M., (2013), "Internal pressure in a low-rise building with existing envelope openings and sudden breaching", *Wind Struct*, **16**(1), 25-46.
Tecle, A.S., Bitsuamlak, G.T., Suskawang, N., Chowdury, A.G. and Fuez, S. (2013), "Ridge and field tile aerodynamics for a low-rise building: a full-scale study", *Wind Struct.*, **16**(4), 301-322.
Van de Lindt, J.W., Graettinger, A., Gupta, R., Skaggs, T., Pryor, S. and Fridley, K.J. (2007), "Performance of wood-frame structures during Hurricane Katrina", *J. Perf. Constr. Facil.*, **21**(2), 108-116.
Vickery, B.J. and Bloxham, C. (1992), "Internal pressure dynamics with a dominant opening", *J. Wind Eng. Ind. Aerod.*, **41**(1-3), 193-204.
Woods, A.R. and Blackmore, P.A. (1995), "The effect of dominant openings and porosity on internal pressures", *J. Wind Eng. Ind. Aerod.*, **57**(2-3), 167-177.
Wu, F.Q. (2000), *Full-scale study of conical vortices and their effects near roof corners*, PhD Thesis, Texas Tech University, Texas.
Zhao, Z.S. (1997), *Wind flow characteristics and their effects on low-rise buildings*, PhD Thesis, Texas Tech University, Texas.

CC